# Study of Polypropylene/Poly(ethylene terephthalate) Bicomponent Melt-Blowing Process: The Fiber Temperature and Elongational Viscosity Profiles of the Spinline

**Ron (Rongguo) Zhao,* Larry C. Wadsworth**

*TANDEC, University of Tennessee, Knoxville, Tennessee 37996*

Received 1 August 2002; accepted 30 September 2002

**ABSTRACT:** Although there are significant differences between high-speed melt spinning and melt blowing (MB), they are similar in many important components. This study, motivated by the need to better understand the bicomponent MB process, used the basic theories of high-speed melt spinning to estimate the fiber temperature and elongation viscosity profiles of the polypropylene/poly(ethylene terephthalate) (PP/PET) bicomponent MB process. During the MB process, the filament temperature decreased dramatically within the first 2 in. from the MB die. The fiber temperature-decay profiles of PP, PET monocomponent, and PP/PET bicomponent filaments followed similar trends. PP filaments attenuated faster than PET filaments and the bicomponent filaments attenuated at a medium rate between that of PP and PET. Accordingly, the elongational viscosity increased significantly in the first 2 in. from the die. PET filaments exhibited higher elongational viscosity than that of 100% PP filaments. The elongational viscosity profile of 75%PP/25%PET was between that of PP and PET monocomponent filaments. These data provided important information on understanding the MB process and filament attenuation. It also suggested that the filament elongational viscosity profile is the key factor in production of finer bicomponent MB fibers. © 2003 Wiley Periodicals, Inc. J Appl Polym Sci 89: 1145–1150, 2003

**Key words:** melt-blowing; viscosity; bicomponent filaments; spinline; high-speed melt spinning

## INTRODUCTION

The spinline dynamics of high-speed melt spinning of several bicomponent polymer systems has been studied by different researchers. Recently Kikutani and colleagues[1] studied high-speed melt spinning of the polypropylene/poly(ethylene terephthalate) (PP/PET) system to investigate the mechanism of fiber structure formation. Radhakrishhan and coworkers[2] studied high-speed melt spinning of both low and high molecular weight PET systems. Radhakrishnan and coworkers[3] also studied ultrahigh-speed spinning of liquid crystalline copolyester with PET, with respect to its fiber structure development, spinnability, and mechanical properties. The filament take-up speed in these studies ranged from 1000 to 8000 m/min.

Although there are significant differences between high-speed melt spinning and melt blowing (MB), they are similar, at least conceptually, in many important components such as the extruder, heater, gear pump, and spinneret. According to Yin et al.,[4] the maximum velocity of MB filament is in the range of 40–70 m/s (2400–4200 m/min) under their experimental conditions. There is no doubt that this number will change with the primary air-jet velocity and it can be much higher depending on the MB die setup and the processing conditions employed, such as airflow rate and air temperature. Therefore, the MB filament velocity can be in the same range as that of regular melt spinning and high-speed melt spinning.

This investigation, motivated by the need to better understand the bicomponent MB process, attempted to use the basic theories of high-speed melt spinning to estimate the fiber temperature and elongation viscosity profiles of PP/PET bicomponent filaments.

### Theory

This study involves two significantly different polymers (PP and PET), which flow side by side through the polymer-distributing coat hanger and each die orifice. To simplify the investigation of the spinline dynamics, a steady-state Newtonian model is assumed for the polymer melt system. The other assumptions include the following: (1) there is no veloc-

*Correspondence to:* R. Zhao (rzhao@biax-fiberfilm.com).

**Present address:* Biax Fiberfilm Corporation, N992 Quality Drive Suite B, Greenville, WI 54942.

Contract grant sponsor: TANDEC, University of Tennessee, Knoxville.

Journal of Applied Polymer Science, Vol. 89, 1145–1150 (2003)

ity gradient in a cross section of the bicomponent filament; (2) the temperatures of the two polymers are identical at a cross section; (3) all extruded polymer is collected on the web-forming collector; (4) the fiber diameter is frozen quickly after being collected at a position in the spinline; (5) the melt temperature at the die is uniform across the die width and equal to the die temperature; and (6) there is no fiber splitting during the MB process.

For this study, the principal equations adapted from melt spinning are the mass balance and energy balance equations, expressed in eqs. (1) and (2), respectively[5]:

$$W = W_{PP,1} + W_{PET,1} = W_{PP,2} + W_{PET,2} \quad (1)$$

$$\frac{dT}{dz} = -\frac{\pi d_f h}{C_{p,PP}W_{PP} + C_{p,PET}W_{PET}}(T - T_a) \quad (2)$$

where $W$, $T$, $z$, and $C_p$ are the mass flow rate, filament temperature, distance from the die, and polymer specific heat, respectively. $T_a$, $h$, and $d_f$ are the air-jet temperature, heat-transfer coefficient, and average filament diameter, respectively. Subscripts 1 and 2 represent the different locations in the spinline. Equation (2) neglects the effects of crystallization during MB processing. By use of the Kase–Matsuo[6] convection model of heat-transfer coefficient, the final energy equation for the MB process is given by[7]

$$\frac{dT_f}{dz} = -\frac{1.652(d_f v_{fa})^{0.334}}{W_{PP}C_p + W_{PET}C_{p,PET}} \times \left(\frac{T_a + T_f}{T_a + T_f + 220.8}\right)^{0.6655}(T_f - T_a) \quad (3)$$

where $T_f$ and $T_a$ are filament and air-jet temperatures, respectively, expressed in K; fiber diameter $d_f$ in m; $W$ in g hole$^{-1}$ s$^{-1}$; $z$ in inch; and $v_{fa}$, the fiber velocity relative to the local air-jet velocity, in m/s. The specific heat $C_p$ of the polymer (J g$^{-1}$ K$^{-1}$) is expressed by the following[1]:

$$C_{p,PP} = 2.72 \quad (4)$$

$$C_{p,PP} = 1.25 + 2.5 \times 10^{-3}T \quad (5)$$

## EXPERIMENTAL

### Polymer materials

1. Exxon PP (ExxonMobil Chemical Co., TX): white pellets with an average size of 3–5 mm in diameter, specially designed for spunbond; nominal melt flow rate (MFR) = 35 g/10 min at 230°C, melting temperature ($T_m$) = 165°C, glass-transition temperature ($T_g$) = −17°C, density ($\rho$) = 0.91 g/cm$^3$.
2. PET (Wellman Inc, SC): semidull fiber grade; intrinsic viscosity (IV) = 0.645 ± 0.017 dL/g; crystallized chip, $T_m$ = 245–250°C; 0.3% $TiO_2$, 2.10 mol % diethylene glycol.

**TABLE I**
**Processing Conditions of Trials for MB Spin-Line Dynamics Study**

| ID | TP (kg/hr) | Air rate (SCFM) | DCD (in.) | PP wt (%) | $T_d = T_a$ (°F) |
|---|---|---|---|---|---|
| Prof-1 | 15 | 350 | 19 | 100 | 599 |
| Prof-2 | 15 | 450 | 19 | 100 | 599 |
| Prof-3 | 7.5 | 450 | 19 | 100 | 599 |
| Prof-4 | 15 | 450 | 19 | 50 | 599 |
| Prof-5 | 15 | 450 | 19 | 25 | 599 |
| Prof-6 | 15 | 450 | 19 | 75 | 599 |
| Prof-7 | 15 | 450 | 15 | 0 | 599 |

### Processing and sample collection

This study was conducted by use of the 24-in. Reicofil MB pilot line made by Reifenhauser (Germany), with a conventional single-row, hole-type die. The die geometry was configured at an air gap of 0.8 mm, a setback of 1.0 mm, and a measured face gap of 1.17 mm (0.0462 in.). A set of MB trials was conducted for the spinline dynamics study. The processing conditions are listed in Table I.

The fibers were collected at different locations along the MB spinline with a specially designed device, which has a 20-in. rigid arm. A driving mechanism was applied to this instrument to ensure the accurate position reading along the spinline and the arm moving speed. A microscope glass slide was attached firmly to the far end of the arm with a proper angle to the air-jet blowing direction. Three fiber-collected slides were produced for each position and properly protected. These samples produced at high arm moving speed were used to determine the average fiber number per in. die width, which were further used to calculate the average fiber velocity.[7] Another set of samples was prepared using the same technique but at a relatively low arm moving speed, which were then used to determine the average fiber diameter. The average of 150 diameter readings of each sample was reported.

A bare thermocouple and a digital thermometer were employed to determine the centerline temperature profile of the air jet. Calibration of the thermometer was carefully performed before the measurements. The polymer flow was turned off and the measurements were conducted until the flow of polymer stopped. To avoid polymer carbonization, the polymer flow was turned on for a proper period of time.

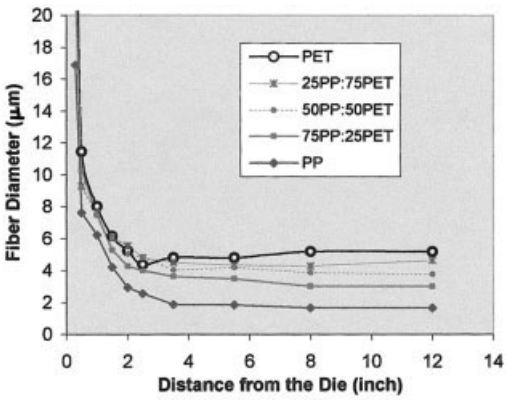


**Figure 1** Fiber diameter profiles of $PP_{35MFR}$, PET, and $PP_{35MFR}$/PET bicomponent MB filaments ($T_a = T_d = 599°F$, TP = 15 kg/h, AR = 450 SCFM, DCD = 19 in., and BS = 54.1 ft/min).

This procedure was repeated as needed. Three readings of air temperature were recorded for each position along the spinline and the average was determined.

## RESULTS AND DISCUSSION

### Fiber diameter profile

The fiber diameter profiles are presented in Figure 1, which compares the fiber attenuation profiles of PP; PET monocomponent MB fiber; and 75%PP/25%PET, 50%PP/50%PET, and 25%PP/75%PET bicomponent MB fibers. It shows that both mono- and bicomponent fiber diameters decreased sharply in the first 2 in. (~ 5 cm) from the die. The filaments of PP attenuated faster than PET filaments and the bicomponent filaments attenuated at a medium rate between that of PP and PET. After the first 2 in. (~ 5 cm), PP filaments continued to decrease in size at a much slower rate until they reached the solidification point, apparently at 4–5 in. (10–13 cm) from the die. The decrease of fiber diameter farther away from this point was minimal. The average diameter of the PET filament decreased continuously up to 2.5 in. (6.3 cm) from the die, after which the fiber diameter exhibited a minor shrinkage-induced increase and stabilized around 8 in. (20.3 cm) from the die.

### Fiber velocity profile

Several techniques were previously used to determine the fiber velocity during melt blowing.[4,8] In this study, fiber velocity, as shown in Figure 2, was calculated from the measured data of fiber diameter, fiber number density, and polymer mass flow rate, based on the mass conservation principle.[7]

Under the experimental conditions, the PP filaments exhibited a maximum velocity of 150 m/s at the position of 3.5 in. (8.9 cm) from the die compared with PET filaments, which were around 70 m/s at 1.5 in. (3.8 cm) from the die. The maximum velocity of 75%PP/25%PET bicomponent filaments, 90 m/s, was between that of PP and PET single-component filaments. After the maximum points, the velocity of PP filament decreased slowly, whereas that of PET dropped sharply.

The air-jet temperature and air velocity profiles were also determined.[7] These profiles were fitted with different equations to best represent the actual measured data and are summarized in Table II. As noticed, the data of each profile are generally fitted with two equations with $R^2$ in the range of 0.9000 to 0.9988.

### Fiber temperature profile

By combining the fitted equations for fiber diameter ($d_f$), fiber velocity ($v_f$), air-jet temperature ($T_a$), and average air velocity ($v_a$), one can estimate the fiber-temperature profile through eq. (3), which is a first-order ordinary differential equation. By providing the following boundary conditions, eq. (3) was solved by use of the powerful MATLAB ODE-solver functions.[7,9]

Boundary conditions for the bicomponent MB process, if the distance from the die $z = 0$ in. (cm) is assumed for each condition, are as follows:

$$T_f = T_{f,0} \tag{6}$$

$$V_f = V_{f,0} \tag{7}$$

$$T_a = T_{a,0} \tag{8}$$

$$V_a = V_{a,0} \tag{9}$$

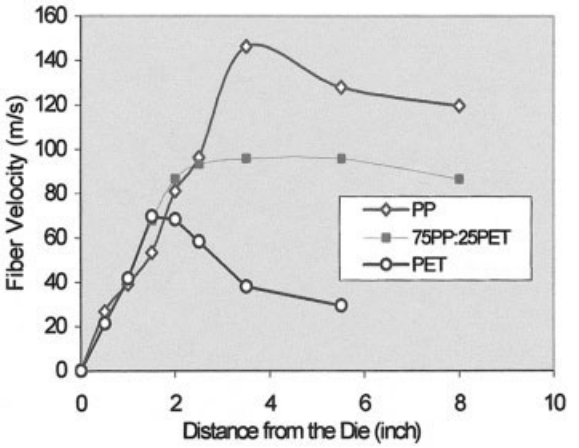


**Figure 2** Fiber velocities of $PP_{35MFR}$, PET, and $PP_{35MFR}$/PET bicomponent MB filaments ($T_d = T_a = 599°F$, TP = 15 kg/h, AR = 450 SCFM, DCD = 19 in., and BS = 54.1 ft/min).

**TABLE II**
**Fitted Equations of the Profiles of Fiber and Air Jet [7]**

| | Equations (unit) | $R^2$ | Range of $z$ (in.)[a] |
|---|---|---|---|
| PP | $d_f = 5.4827 \times 10^{-6} z^{-0.8372}$ (m) | 0.9704 | 0–5.5 |
| | $d_f = (0.0104z^2 - 0.2113z + 2.6868) \times 10^{-6}$ (m) | 1.0 | 5.5–10 |
| | $v_f = 40.293z - 0.0305$ (m/s) | 0.9898 | 0–3.5 |
| | $v_f = 197.35z^{-0.245}$ (m/s) | 0.9815 | 3.5–10 |
| PET | $d_f = 8.786 \times 10^{-6} \times z^{-0.8436}$ (m) | 0.92480 | 0–2.5 |
| | $d_f = 4.0901 \times 10^{-6} \times z^{-0.1021}$ (m) | 8626 | 2.5–10 |
| | $v_f = 44.803z$ (m/s) | 0.9936 | 0–1.5 |
| | $v_f = 104.11z^{-0.7402}$ (m/s) | 0.9410 | 1.5–10 |
| 25PP/75PET | $d_f = 8.0697 \times 10^{-6} \times z^{-0.7114}$ (m) | 0.8515 | 0–2.5 |
| | $d_f = 5.1559 \times 10^{-6} \times z^{-0.0956}$ (m) | 0.8911 | 2.5–10 |
| | $v_f = -11.293z^2 + 56.571z$ (m/s) | 0.9836 | 0–2.5 |
| | $v_f = -0.7469z^2 + 4.8143z + 67.655$ (m/s) | 0.9385 | 2.5–10 |
| 50PP/50PET | $d_f = 7.8641 \times 10^{-6} \times z^{-0.7845}$ (m) | 0.8578 | 0–2.0 |
| | $d_f = 5.2916 \times 10^{-6} \times z^{-0.1539}$ (m) | 0.6368 | 2.0–10 |
| | $v_f = -5.9025z^2 + 45.31z$ (m/s) | 0.9825 | 0–3.5 |
| | $v_f = 1.1501z^2 - 16.218z + 131.14$ (m/s) | 1.0 | 3.5–10 |
| 75PP/25PET | $d_f = 7.22 \times 10^{-6} \times z^{-0.7942}$ (m) | 0.9641 | 0–2.5 |
| | $d_f = 4.8259 \times 10^{-6} \times z^{-0.205}$ (m) | 0.9503 | 2.5–10 |
| | $v_f = 40.587z$ (m/s) | 0.9825 | 0–3.5 |
| | $v_f = -0.8192z^2 + 7.403z + 79.775$ (m/s) | 0.9988 | 2.5–10 |
| Air Jet | $T_a = T_{a,0}$ (°F) | — | $z \leq 3.5w$ |
| | $T_a = 1.79(T_{a,0} - T_\infty)(w/z)^{0.465} + T_\infty$ (°F) | — | $z > 3.5w$ |
| | $V_a = V_{a,0}$ (m/s) | — | $z \leq 8.6w$ |
| | $V_a = 2.92V_{a,0}(w/z)^{0.5}$ (m/s) | — | $z > 8.6w$ |

[a] $z$; the distance from the die; $w$; face gap (0.0462 in.).

$$d_f = d_{f,0} \tag{10}$$

The calculated fiber-temperature profiles are presented in Figure 3. One finds that the fiber temperature decreases dramatically in the first 2 in. Because of the higher temperature gradient near the die and a significant amount of secondary air drawn from ambient conditions, heat radiation and convection are the two main driving mechanisms of the temperature drop of the air jet and the fiber. Interestingly, under the same processing conditions, the temperature profiles of both mono- and bicomponent MB fibers appear almost identical, as shown in Figure 3. However, a closer examination of Figure 4 reveals that 100% PET filaments exhibit the lowest temperature compared to that of single $PP_{35MFR}$ and $PP_{35MFR}$/PET bicomponent filaments. The maximum difference for single PP and single PET filaments is between 2 and 5°C, which is expected to be even smaller among the filaments with different polymer ratios. This result may be balanced by the differences in fiber diameter and fiber velocity of the filaments with different component ratios. For

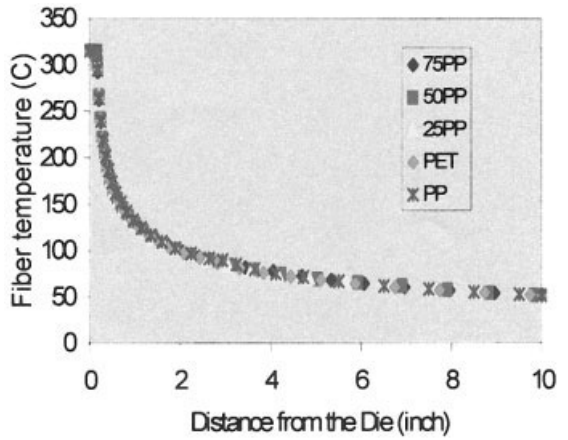


**Figure 3** Fiber temperature profiles of $PP_{35MFR}$, PET, and $PP_{35MFR}$/PET bicomponent filaments.

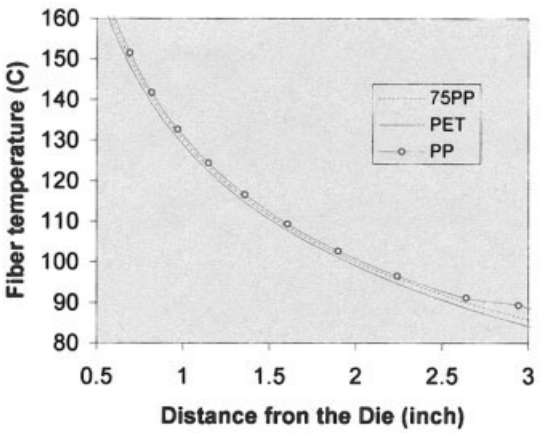


**Figure 4** Close-up of the calculated temperature profiles of $PP_{35MFR}$, PET, and $PP_{35MFR}$/PET bicomponent filaments.

example, the PP filament is attenuated to a much lower fiber diameter, which improves the heat transfer from the center to the surface of the fiber; thus, its temperature decreases more quickly. On the other hand, the PET filament is less attenuated, which results in larger fiber size and exhibits lowered efficiency of heat loss.

At a crystallization temperature around 150–165°C, the PP phases of the PP/PET bicomponent filaments were expected to start crystallizing at 0.6 in. (1.5 cm) from the die. The air drag on the filaments could significantly enhance polymer molecular orientation and the crystallization of PP. At a distance of 2.08 in. from the die, the average temperature of 75%$PP_{35MFR}$/25%PET bicomponent filaments was calculated to be about 99°C. Although PET is the predominant component, the filaments exhibited a smooth attenuation profile without a shrinkage-induced fiber diameter increase as that of single PET filaments. This observation could result partially from the quick crystallization of the $PP_{35MFR}$ phase in the bicomponent filaments.

### Elongational viscosity profile

Melt blowing is a continuous, uniaxial-stretching–like operation, where elongational viscosity ($\eta_e$) is a critical property for better understanding the process. Estimating $\eta_e$ from the Newtonian shear viscosity was first attempted by Trouton[10] by the following formula:

$$\eta_e = 3\eta_0 \tag{11}$$

where $\eta_0$ is the zero shear Newtonian viscosity. This relation was previously found not to be rigorously correct for many cases.[11] By assuming a Newtonian flow behavior, Haynes[12] used the following equation for elongational viscosity of PP in his research of the MB process:

$$\eta_e = 2\eta_0 \tag{12}$$

In this study, zero shear viscosities of PP [MFR = 35 g/10 min (35 MFR)] at higher temperatures were determined by extrapolating the viscosity to a rate of zero. These data were combined with Patel's data for a PP of 35 MFR[13] and eq. (12). The following Arrhenius model of elongational viscosity (in Pa·s) was then developed and given by[7]

$$\eta_{e,PP} = 2.56 \times 10^{-4} \exp\left(\frac{7316}{T + 273}\right) \tag{13}$$

The elongational viscosity of PET (in Pa·s) is a function of temperature and molecular weight, given as follows[2]:

$$\eta_{e,PET} = 0.3[IV]^{5.1} \exp\left[2.303\left(\frac{3280}{T + 273}\right) - 1.54\right] \tag{14}$$

where IV is intrinsic viscosity (in dL/g). In eqs. (13) and (14), the temperature $T$ is in °C.

The PET used in this study has an IV of 0.645 dL/g. With the fiber temperature profile results and eqs. (13) and (14), it is not difficult to find the elongational viscosity profiles of PP and PET, as shown in Figure 5. Under the experimental conditions, the elongation viscosity of PET was estimated to be five to ten times higher than that of $PP_{35MFR}$ at all locations in the spinline. This gives a direct explanation of the results that 100% PET filaments are larger in diameter than are 100% PP filaments, as observed in Figure 1. The nature of the polymer determines the elongational viscosity at a given processing condition. Therefore, the higher final fiber diameter of PET is a natural result compared with the much finer fiber size of $PP_{35MFR}$. If one assumes that the average elongational viscosity of a bicomponent (bico) MB filament obeys the simple rule of mixtures, it can be estimated by use of the following expression:

$$\eta_{e,bico} = W_{PP}\%\eta_{e,PP} + W_{PET}\%\eta_{e,PET}$$

As shown in Figure 5, the estimated average viscosity of 75%$PP_{35MFR}$/25%PET bicomponent filament lies between that of PP and PET monocomponent filaments. The PET component significantly increased the elongational viscosity of the bicomponent filament, resulting in higher resistance to the attenuation force and higher average final fiber diameter compared with that of 100% PP MB fiber. With more PET in the filament, a higher $\eta_e$ is expected, and a consequently larger fiber size is not surprising, as observed in Figure 1. After the polymer melts were extruded from the die, $\eta_e$ increased dramatically within the first 2 in. (5 cm) from the die tip. Thereafter, at a certain location in the spinline, $\eta_e$ reached a level that the local air-drag

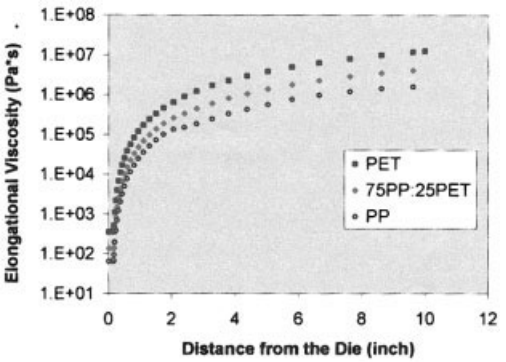


**Figure 5** Elongational viscosity of $PP_{35MFR}$, PET, and $PP_{35MFR}$/PET bicomponent MB filaments ($T_a = T_d$ = 315°C, TP = 15 kg/h, AR = 450 SCFM, DCD = 19 in.).

force was no longer strong enough to attenuate the filament. In PET melt spinning with an intermediate take-up speed, its $T_g$ (71°C) was taken as the solidification temperature.[11] Because no positive drawing device is available in MB processing, the solidification temperature for PET MB filament is, of course, higher than its $T_g$. If the transition point in the fiber diameter profile is taken as the solidification point (2.5 in. from the die), the solidification temperature of PET MB filament can be estimated from Figure 4 as about 92°C, which corresponds to an elongational viscosity of about $9.8 \times 10^5$ Pa·s. For the $PP_{35MFR}$/PET bicomponent filaments, it is reasonable to assume that the fiber attenuates continuously until the average $\eta_e$ reaches this value. Therefore, the solidification point in the spinline for bicomponent filaments lies farther from the MB die, as shown in Figure 1. Compared with the PET single-component filament, the PP component improved the filament attenuation of the bicomponent filament and increased the bonding property of the web, and thus enhanced its processability.

## CONCLUSIONS

During the melt-blowing process, the filament temperature decreased dramatically within the first 2 in. (5 cm) from the MB die. The fiber temperature-decay profiles of PP, PET monocomponent, and PP/PET bicomponent filaments followed similar trends. PP filaments attenuated faster than PET filaments and the bicomponent filaments attenuated at a medium rate between that of PP and PET; the elongational viscosity increased significantly in the first 2 in. (5 cm) from the die. PET filaments exhibited much higher elongational viscosity than that of 100% PP filaments. The elongational viscosity profile of 75%PP/25%PET was between that of PP and PET monocomponent filaments. These data provided important information on understanding the MB process and filament attenuation. It also suggested that the filament elongational viscosity profile is the key factor in production of finer bicomponent MB fibers.

The first author is grateful to Drs. Larry C. Wadsworth and David Garner for encouragement and guidance during this study. He also thanks TANDEC, University of Tennessee, Knoxville for generous financial support to this project. Exxon Chemical Company is highly appreciated for providing polypropylene resins.

## References

1. Kikutani, T.; Radhakrishnan; Arikawa, S.; Takaku, A.; Okui, N.; Jin, X.; Niwa, F.; Kudo, Y. J Appl Polym Sci 1996, 62, 1913.
2. Radhakrishhan, J.; Kikutani, T.; Okui, N. Textile Res J 1997, 67, 684.
3. Radhakrishhan, J.; Ito, H.; Kikutani, T.; Okui, N. Polym Eng Sci 1999, 39, 89.
4. Yin, H.; Yan, Z.; Bresee, R. R. Int Nonwovens J 1999, 8, 60.
5. Ziabicki, A.; Kawai, H., Eds. High-speed Fiber Spinning: Science and Engineering Aspects; Wiley: New York, 1985.
6. Kase, S.; Mastsuo, T. J Polym Sci 1965, A-3, 2541.
7. Zhao, R. Ph.D. Dissertation, University of Tennessee, Knoxville, 2001.
8. Wu. T. T.; Shambaugh, R. L. Ind Eng Chem Res 1992, 31, 379.
9. Pratap, R. Getting Started with Matlab 5; Oxford University Press: New York, 1999; pp. 128–137.
10. Han, C. D. Rheology in Polymer Processing; Academic Press: New York, 1976; p. 198.
11. George, H. H. Polym Eng Sci 1982, 22, 292.
12. Haynes, B. D. Ph.D. Dissertation, The University of Tennessee, Knoxville, 1991.
13. Patel, R. M.S. Thesis, University of Tennessee, Knoxville, 1988.